Motion of two superposed viscous fluids

Andrea Prosperetti

Istituto di Fisica, Universita di Milano, Milano, Italy

The initial-value problem associated with the small-amplitude waves on the interface between two superposed viscous fluids is studied in the stable and in the unstable case (Rayleigh–Taylor instability). The results are illustrated with examples obtained by numerical and analytic inversion of the Laplace-transformed solution for the wave amplitude. The diffusion of vorticity from the free surface into the fluids is also shown.

I. INTRODUCTION

The classic problem of the small-amplitude motion of two superposed viscous fluids has recently been considered as an initial-value problem[1,2] rather than in a normal-mode (or eigenvalue problem) framework as, with only one exception,[3] had been done in the past (see, e.g., Ref. 4, p. 625, Ref. 5, Chap. X, and Refs. 6–10). This new approach has elucidated several features of the process connected with the transition from the initial behavior to a single-mode growth or decay for large times.[1] A prominent role in this transition is played by the continuous part of the spectrum of the associated eigenvalue problem. Curiously enough, this part of the spectrum, although commonly encountered in other branches of mathematical physics (notably quantum mechanics[11]), has never received great attention in fluid mechanics, and it is only recently that its effect and characteristics have begun to be investigated for problems of this type[1–3,12,13] as well as of another nature.[14]

It is well known that when the upper fluid is denser than the lower one, the system is unstable for sufficiently long wavelengths. This situation, which continues to be of research interest in other contexts,[15–17] is usually referred to as the Rayleigh–Taylor instability. The converse configuration in which the lower fluid is denser is a stable one, and the interface motion consists of damped oscillations.

In this study we consider the linearized initial-value problem for both the stable and the unstable case. For simplicity, we assume that the initial vorticity vanishes. The only sources of vorticity for the system are then the boundary conditions at the interface.[1,18] As discussed in Ref. 1, this surface-generated vorticity diffuses into the body of the fluids until a pseudo-steady distribution is reached, which corresponds analytically to the situation described by the least damped normal-mode solution. The effects of a nonzero initial vorticity are considered in Refs. 2 and 19.

The analysis leads to a solution in terms of Laplace transforms which can be inverted analytically in only three special cases. For the other cases, we present results obtained by means of numerical inversion of the transform. We also include a detailed comparison of our exact solution with the ones obtained by means of the normal-mode analysis and, where appropriate, of the irrotational approximation.

II. FORMULATION AND SOLUTION

We consider two superposed viscous, incompressible fluids of infinite depth and lateral extent. Quantities pertaining to the upper and lower fluids are denoted by the subscripts u and l, respectively. Equations in which no subscript appears hold indifferently for both media. At equilibrium, the interface of the two fluids occupies a plane which we take as the (x, z) plane. The vertical axis, y, is oriented from the lower to the upper fluid against the direction of gravity.

Since we are going to restrict our considerations to the linearized case, we can, by means of a Fourier analysis, limit our study to waves of specified wavenumber $k = (k_x^2 + k_z^2)^{1/2}$, where k_x and k_z are the components of the wave vector in the plane. Accordingly, we write the equation of the free surface in the following form appropriate for standing waves

$$y = a(t) f(x, z), \tag{1}$$

where the function f satisfies the Helmholtz equation in the plane $(\partial_x^2 + \partial_z^2 + k^2) f = 0$. On either side of the interface the motion of the fluids is governed by the linearized Navier–Stokes equations and the solenoidal constraint on the velocity field. At the interface the standard kinematic condition and the conditions of continuity of tangential velocity and tangential stresses are applied, while the discontinuity in the normal stresses is required to be balanced by the effect of surface tension.

In order to solve the problem we eliminate the pressure by taking the curl of the linearized Navier–Stokes equation to obtain

$$\frac{\partial \omega}{\partial t} = \nu \nabla^2 \omega, \tag{2}$$

where ω is the vorticity and ν is the kinematic viscosity. Since by definition $\nabla \cdot \omega = 0$, we can introduce a vector potential for the vorticity, which we write as

$$\omega = \nabla \times (\mathbf{A} + \nabla \times \mathbf{B}). \tag{3}$$

This form is particularly convenient since it can be shown[2,20] that a suitable gauge transformation allows the fields $\mathbf{A}$ and $\mathbf{B}$ to be taken as oriented along the y axis,

$$\begin{aligned} \mathbf{A} &= [0, \Omega(y, t) f(x, z), 0], \\ \mathbf{B} &= [0, G(y, t) f(x, z), 0]. \end{aligned} \tag{4}$$

Definitions (3) and (4) are similar to the decomposition of a solenoidal field into a toroidal and a poloidal

component on a sphere (Ref. 5, Appendix III). The relation between the fields A, B and the velocity u is clearly of the form

$$u = A + \nabla \times B - \nabla \phi . \tag{5}$$

The scalar potential ϕ is necessary in order to satisfy the condition of incompressibility which, from (5), is seen to require

$$\nabla^2 \phi = \nabla \cdot A . \tag{6}$$

Upon substitution of (5) into the linearized Navier–Stokes equation and integration it is possible to obtain the following Bernoulli-like equation for the pressure field p[2,20]

$$p = -\rho g y + \frac{\partial \phi}{\partial t} - \nu \frac{\partial \Omega}{\partial y} f , \tag{7}$$

where ρ is the density and g is the magnitude of the gravitational acceleration.

Inserting (3) into (2) we obtain, after some obvious manipulations,

$$\left[\frac{\partial}{\partial t} - \nu\left(\frac{\partial^2}{\partial y^2} - k^2 \right) \right] \Omega = 0 , \tag{8}$$

with an identical equation for G, while (6) gives

$$\left(\frac{\partial^2}{\partial y^2} - k^2 \right)\Phi = \frac{\partial \Omega}{\partial y} , \tag{9}$$

where $\phi = \Phi(y, t) f(x, z)$. The general integral of this equation can readily be obtained by Lagrange's method of variation of parameters. Substitution of the results into (7) gives the following expression for the pressure fields:

$$p_l = -\rho_l g y - [k\mu_l \Omega_l(0, t) + \rho_l k^{-1}\ddot{a}] e^{ky} f(x, z) ,$$
$$p_u = -\rho_u g y + [k\mu_u \Omega_u(0, t) + \rho_u k^{-1}\ddot{a}] e^{-ky} f(x, z) , \tag{10}$$

where the dots denote differentiation with respect to time. The continuity of tangential velocities is readily seen to require that

$$\int_{-\infty}^0 \Omega_l e^{ky} dy + \int_0^\infty \Omega_u e^{-ky} dy = 2k^{-1}\dot{a} , \tag{11}$$

$$G_u(0, t) = G_l(0, t) \tag{12}$$

and the continuity of tangential stresses that

$$\mu_u \Omega_u(0, t) - \mu_l \Omega_l(0, t) = 2(\mu_u - \mu_l)\dot{a} , \tag{13}$$

$$\left(\frac{\partial}{\partial y} (\mu_u G_u - \mu_l G_l) \right)_{y=0} = 0 . \tag{14}$$

Finally, the condition on the normal stresses gives

$$(\rho_u + \rho_l)\ddot{a} + 2k^2(\mu_u + \mu_l)\dot{a} + (\rho_u + \rho_l)\omega_0^2 a$$
$$+ k^2\mu_l\left(\Omega_l(0, t) - 2k \int_{-\infty}^0 \Omega_l e^{ky} dy \right)$$
$$+ k^2\mu_u\left(\Omega_u(0, t) - 2k \int_0^\infty \Omega_u e^{-ky} dy \right) = 0 . \tag{15}$$

Here, ω_0 is the inviscid natural frequency given by (see Ref. 4, p. 370)

$$\omega_0^2 = \frac{\rho_l - \rho_u}{\rho_l + \rho_u} gk + \frac{\zeta}{\rho_l + \rho_u} k^3 . \tag{16}$$

The system considered is stable or unstable according as $\omega_0^2 > 0$ or $\omega_0^2 < 0$. The latter case is only possible if the upper fluid is denser than the lower one, and for wavenumbers smaller than a cutoff wavenumber k_c given by[3,5,9] $k_c = [(\rho_u - \rho_l)g/\zeta]^{1/2}$.

Notice that the problem for the component G of the vorticity is effectively uncoupled from that involving Ω and a. This is intuitively clear, since it is seen from (5) that this component describes rotational motion in the (x, z) planes and, therefore, it would be needed only to accommodate particular initial conditions. For $t > 0$, however, it would evolve independently of the Ω component and of the free-surface elevation. Since we have assumed zero initial vorticity, this component also remains zero for $t > 0$ and we can disregard it.

III. EQUATION OF MOTION OF THE INTERFACE

The system of equations (8), (11), and (13) can be solved using the Laplace transform with the result

$$\tilde{\Omega}_l = -2(\lambda_l + k) \frac{\mu_l k + \mu_u \lambda_u}{\mu_l(\lambda_l + k) + \mu_u(\lambda_u + k)} \exp(\lambda_l y)\tilde{a} ,$$
$$\tilde{\Omega}_u = -2(\lambda_u + k) \frac{\mu_u k + \mu_l \lambda_l}{\mu_l(\lambda_l + k) + \mu_u(\lambda_u + k)} \exp(-\lambda_u y)\tilde{a} , \tag{17}$$

where the tilde indicates the transformed function, s is the variable conjugate to time, and

$$\lambda_{l,u} = (k^2 + s/\nu_{l,u})^{1/2} .$$

The expressions (17) can be substituted into (15) to obtain an integrodifferential equation of motion for the amplitude of the surface displacement. In the time domain this equation can be written out explicitly only in the limiting cases in which only one fluid has appreciable dynamical effects (i.e., either $\rho_l = \mu_l = 0$ or $\rho_u = \mu_u = 0$), or when the fluids have equal kinematical viscosities, $\nu_l = \nu_u$. In the first instance one finds

$$\ddot{a} + 4k^2\nu_{l,u}\dot{a} + \omega_0^2 a$$
$$- 4k^3\pi^{-1/2}\nu_{l,u}^{3/2} \int_0^t \{\tau^{-1/2} \exp(-k^2\nu_{l,u}\tau)$$
$$- k(\pi\nu_{l,u})^{1/2} \text{erfc}[k(\nu_{l,u}\tau)^{1/2}]\} \dot{a}(t - \tau)d\tau = 0 . \tag{18}$$

The stable and unstable cases differ only in the sign of ω_0^2. The terms containing $\dot{a}$, which describe the damping of the system, are identical in the two cases. The first of these terms, simply proportional to $\dot{a}$, corresponds to the surface contribution to energy dissipation [see Ref. 4, p. 581, Eq. (12)], while the second one describes the dissipation taking place in the body of the fluid. Notice that, for the case of small viscosity, this term is a factor of $\nu^{1/2}$ smaller than the other one, and hence, as a first approximation, it can be neglected. Thus, as is well known, for $\nu \to 0$ it is possible, to leading order, to estimate the dissipation rate by means of the irrotational solution (see Ref. 4, p. 623). As clearly explained by Batchelor[18] this procedure is correct in these cases because the condition of vanishing tangential stress at the free surface leads to a much weaker vorticity generation than a no-slip condition. This aspect is clearly illustrated by contrasting Eq. (18) with that found for the two-fluid, equal ν case for which the corresponding

equation is

$$\ddot{a} + 2\nu k^2 \left(1 + \frac{\rho_u^2 + \rho_l^2}{(\rho_u + \rho_l)^2}\right)\dot{a} + \omega_0^2 a$$

$$- \frac{2k\rho_l\rho_u}{(\rho_u + \rho_l)^2}\left(\frac{\nu}{\pi}\right)^{1/2}\int_0^t \tau^{-3/2}\exp(-k^2\nu\tau)\dot{a}(t-\tau)d\tau$$

$$+ 4k^3\left(\frac{\rho_u - \rho_l}{\rho_u + \rho_l}\right)^2 \frac{\nu^{3/2}}{\pi^{1/2}}\int_0^t \{k(\pi\nu)^{1/2}\,\mathrm{erfc}[k(\nu\tau)^{1/2}]$$

$$- \tau^{-1/2}\exp(-k^2\nu\tau)\}\dot{a}(t-\tau)dt = 0 . \tag{19}$$

The extra integral term appearing here in comparison with (18) is a direct consequence of the condition of continuity of tangential velocity which applies when both fluids have appreciable dynamical effects. Notice that, for $\nu \to 0$, this term is the leading one in describing the energy dissipation of the motion. Therefore, use of the inviscid potential flow solution in this case would give incorrect results for the damping of the wave even when the viscosity is small.

Equations (18) and (19) can be solved in closed form. For both cases the result can compactly be written as[1,2]

$$a(t) = \frac{4(1 - 4\beta)\nu^2 k^4}{8(1 - 4\beta)\nu^2 k^4 + \omega_0^2}\,a_0\,\mathrm{erfc}(\nu k^2 t)^{1/2}$$

$$+ \sum_{i=1}^{4}\frac{z_i}{Z_i}\left(\frac{\omega_0^2 a_0}{z_i^2 - \nu k^2} - u_0\right)$$

$$\times \exp[(z_i^2 - \nu k^2)t]\,\mathrm{erfc}(z_i t^{1/2}) , \tag{20}$$

where the z_i's are the four roots of the algebraic equation

$$z^4 - 4\beta(k^2\nu)^{1/2}z^3 + 2(1 - 6\beta)k^2\nu z^2$$

$$+ 4(1 - 3\beta)(k^2\nu)^{3/2}z + (1 - 4\beta)\nu^2 k^4 + \omega_0^2 = 0 , \tag{21}$$

and $Z_1 = (z_2 - z_1)(z_3 - z_1)(z_4 - z_1)$ with Z_2, Z_3, Z_4 obtained by circular permutation of the indices. The dimensionless parameter β is given by $\beta = \rho_l\rho_u/(\rho_l + \rho_u)^2$ and is zero in the one-fluid cases. Furthermore, $a_0 = a(0)$ and $u_0 = \dot{a}(0)$.

Notice that, if one writes $\mathrm{erfc}x = 1 - \mathrm{erf}x$, Eq. (20) becomes the sum of four exponentials, plus other more complicated terms. From a normal-mode point of view, the exponentials would be the contribution of the discrete spectrum, while the other terms would arise from the continuous spectrum.[21]

The cases for which we have presented the explicit result (20) appear to be the only ones in which it is possible to obtain a closed-form solution for a in the time domain. In general, it is only possible to solve for the Laplace-transformed function $\bar{a}(s)$. The result is

$$\bar{a}(s) = \frac{1}{s}\left(a_0 + \frac{su_0 - \omega_0^2 a_0}{s^2 + \Lambda(s)s + \omega_0^2}\right). \tag{22}$$

The function $\Lambda(s)$ describes the dissipation and is given by

$$\Lambda = 4k\{-\rho_l\rho_u s + k(\mu_u - \mu_l)[\rho_u(k - \lambda_l) - \rho_l(k - \lambda_u)]$$

$$+ k^2(\mu_l - \mu_u)^2(k - \lambda_l)(k - \lambda_u)s^{-1}\}$$

$$\times \{(\rho_l + \rho_u)[\rho_l(k - \lambda_u) + \rho_u(k - \lambda_l)]\}^{-1} . \tag{23}$$

Notice that $\Lambda = 0$ when both μ_l and μ_u vanish and that its value does not change if the physical properties of the upper and lower fluids are interchanged.

In the same way as in Ref. 21, or by formally inverting the Laplace transform (22), it is possible to show that the asymptotic behavior of the solution in the time domain is, for $t \to \infty$,

$$a(t) \simeq \frac{u_0\sigma - \omega_0^2 a_0}{\sigma[2\sigma + \Lambda(\sigma) + \Lambda'(\sigma)\sigma]}\,e^{\sigma t} , \tag{24}$$

where σ is the root of

$$\sigma^2 + \Lambda(\sigma)\sigma + \omega_0^2 = 0 , \tag{25}$$

with the largest real part. In the normal-mode approach, Eq. (25) is just the characteristic equation for the discrete spectrum and (24) exhibits the typical exponential time dependence. Notice that, in this approach, the constant multiplying the exponential should be obtained by means of a scalar product in a suitable Hilbert space, but has never been written down explicitly in view of the rather complex calculation required to obtain it in this way.

IV. RESULTS: UNSTABLE CASE

For a discussion of the results for the unstable case it is useful to make use of the nondimensional variables introduced in Ref. 22 on the basis of a fundamental length L, time T, and mass M given by

$$L = \left(\frac{\bar{\nu}^2}{Ag}\right)^{1/3} , \quad T = \left(\frac{\bar{\nu}}{A^2 g^2}\right)^{1/3} , \quad M = \frac{\bar{\nu}^2(\rho_l + \rho_u)}{Ag} , \tag{26}$$

where $A = (\rho_u - \rho_l)/(\rho_u + \rho_l)$ and $\bar{\nu} = (\mu_u + \mu_l)/(\rho_u + \rho_l)$. Variables made dimensionless with respect to these fundamental quantities will be denoted by an asterisk in the following. In particular, for the surface tension parameter we have $\zeta^* = (Ag\bar{\nu}^4)^{-1/3}(\rho_l + \rho_u)^{-1}\zeta$, and $\omega_0^{*2} = -k^*(1 - \zeta^*k^{*2})$. As other parameters to characterize the properties of the two fluids we take

$$A_{l,u} = \frac{\rho_{l,u}}{\rho_l + \rho_u} , \quad C_{l,u} = \frac{\mu_{l,u}}{\mu_l + \mu_u} ; \tag{27}$$

clearly, $A_l + A_u = C_l + C_u = 1, A_u - A_l = A$.

In view of its physical interest (and to reduce the number of independent parameters) we shall present results only for the [asymptotically, cf. Eq. (24)] fastest growing wavelength, which has been shown, in Ref. 22, to be given within a few percent by the simple approximate formula

$$(k^*_{max})^{-1} = \tfrac{3}{4}(4 + 3\zeta^*)^{1/2} + \tfrac{1}{4}(3\zeta^*)^{1/2} + 0.47 , \tag{28}$$

for all values of $A_{l,u}, C_{l,u}$. We have used this approximate expression for the selection of the wavenumber directly without further corrections, since it is known that the maximum in the $\sigma - k$ curve is rather broad.[22] For a graph of this relation the reader is referred to Fig. 4 of Ref. 22; k^*_{max} decreases with increasing ζ^*.

Let us first consider the case in which the lower fluid is absent, for which we have the explicit result (20) with $\beta = 0$. As shown in Ref. 1 in this case an approximation valid for small time, irrespective of the value of the viscosity, (or, more precisely, for small values

of $\nu k^2 t$) can be obtained from the irrotational result, which amounts to omitting the integral term in (18). Thus, we find (in dimensional variables)

$$a(t) \simeq (\sigma_2 - \sigma_1)^{-1}[(\sigma_2 a_0 - u_0)e^{\sigma_1 t} - (\sigma_1 a_0 - u_0)e^{\sigma_2 t}], \qquad (29)$$

where $\sigma_{1,2} = 2\nu_u k^2 \pm [k(g - \zeta k^2/\rho_u)]^{1/2}$. In Figs. 1–3 we compare the exact result (20) (continuous line) with the asymptotic approximation (24) (dashed line) and this initially-valid irrotational approximation (dash-and-dot line) for values of ζ^* of 0.01, 1, and 1000, respectively. The corresponding values of k^*_{max} are 0.4953, 0.3463, and 0.01809. For all cases we have taken the initial conditions $a_0 = 1$, $u_0 = 0$.

Here and in the following, ζ^* can be considered a measure of the viscosity of the system, viscous effects becoming more important as ζ^* decreases. For a better quantitative measure of the effect of viscosity we may use the dimensionless quantity

$$\epsilon = \frac{\nu k^2}{|\omega_0^2|^{1/2}} = \frac{k^{*2}}{(k^* - \zeta^* k^{*3})^{1/2}}, \qquad (30)$$

which represents the ratio of the time for the disturbance to be amplified by a factor of order e to the time required for viscous effects to propagate into the fluid to a depth of order λ. Clearly, viscous effects are negligible for ϵ near zero (for an air-water configuration in normal gravity, for example, $\zeta^* \simeq 3400$ and $\epsilon \simeq 1.2 \times 10^{-3}$), whereas they tend to become important as ϵ increases. For the examples of Figs. 1–3 we have $\epsilon = 0.349$, 0.217, and 2.97×10^{-3}, respectively.
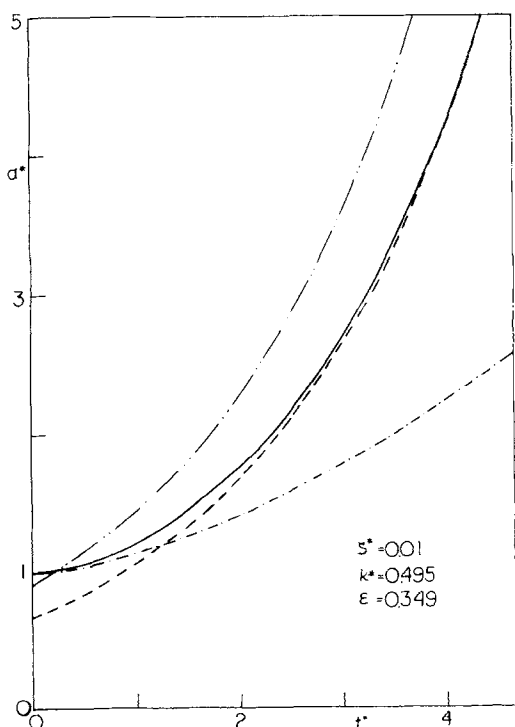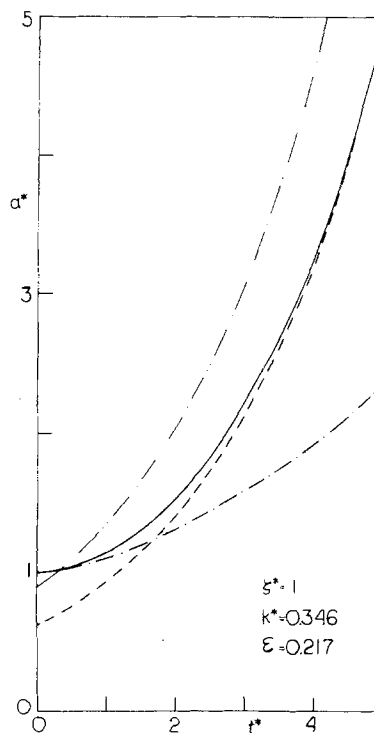
FIG. 2. The amplitude of the free surface motion in the unstable, one-fluid case [Eq. (20), continuous line] is compared with the asymptotic, normal mode result [Eq. (24), dashed line], the initially valid, irrotational approximation [Eq. (29), dash-and-dot line], and the mixed approximation of Eq. (31) (dash-double dot line) for $a_0 = 1$, $u_0 = 0$, $k^* = 0.346$, $\zeta^* = 1$.
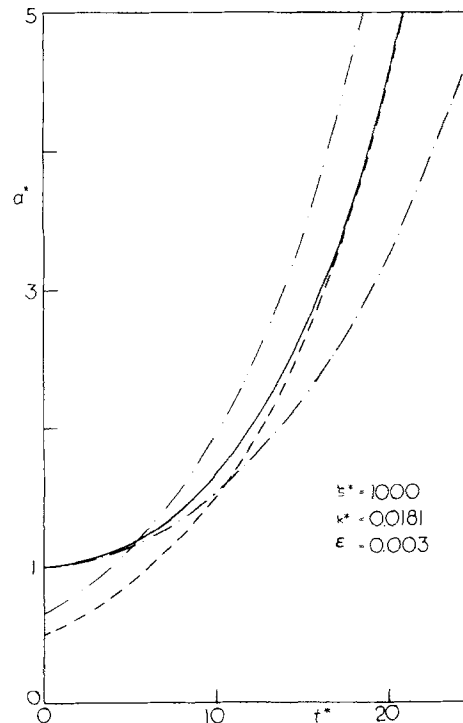
FIG. 1. The amplitude of the free surface motion in the unstable, one-fluid case [Eq. (20), continuous line] is compared with the asymptotic, normal mode result [Eq. (24), dashed line], the initially valid, irrotational approximation [Eq. (29), dash-and-dot line], and the mixed approximation of Eq. (31) (dash-double dot line) for $a_0 = 1$, $u_0 = 0$, $k^* = 0.495$, $\zeta^* = 0.01$. The lower fluid is absent.

FIG. 3. The amplitude of the free surface motion in the unstable, one-fluid case [Eq. (20), continuous line] is compared with the asymptotic, normal mode result [Eq. (24), dashed line], the initially valid, irrotational approximation [Eq. (29), dash-and-dot line], and the mixed approximation of Eq. (31) (dash-double dot line) for $a_0 = 1$, $u_0 = 0$, $k^* = 0.0181$, $\zeta^* = 1000$.
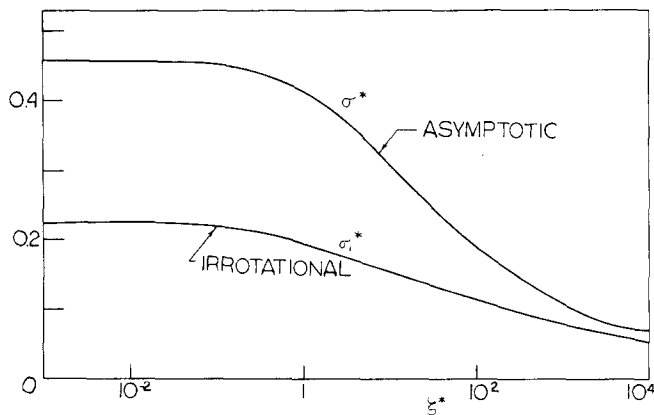
FIG. 4. Comparison of the dimensionless asymptotic growth rate, given by Eq. (25), with the irrotational growth rate of Eq. (29) for the one-fluid, unstable case, as functions of the dimensionless surface tension parameter ζ^* for $k^* = k^*_{max}$.

The examples shown clearly exhibit the mutual relation between the approximate and the exact result. The rate at which the initial behavior departs from the latter increases with viscosity, and likewise the rate at which this result approaches the asymptotic one increases with viscosity. Although, as already explained, these figures correspond to different values of k^*, the same behavior was observed in a limited number of other studies in which k^* was varied keeping ζ^* fixed. In Fig. 4 we present a comparison of the dimensionless asymptotic growth rate σ^* and the irrotational one, σ^*_1, as a function of ζ^*. It is clear that, as pointed out in Ref. 9, the irrotational approximation is always more damped than the asymptotic result. This circumstance is caused by the fact that, near the free surface, the irrotational motion has much steeper velocity gradients than the viscous one.

It is obvious that a single exponential like (24) cannot be made to fit both initial conditions at $t = 0$. The particular choice of the multiplicative constant made in (24) ensures asymptotic agreement with the exact result, but then both initial conditions are violated. An alternative approach might be to use the multiplicative constant of the irrotational approximation (29), in combina-
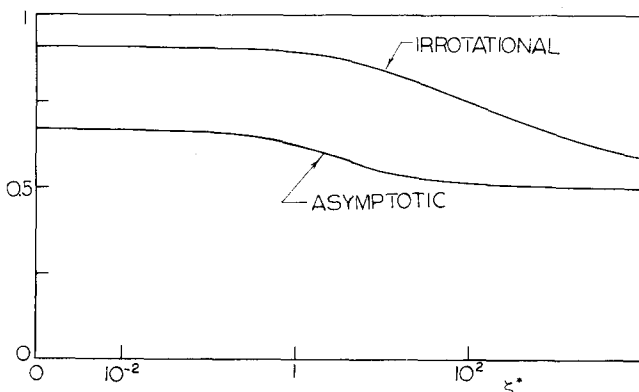

FIG. 5. Comparison of the multiplicative constants in front of the exponentials in Eqs. (24) and (29) for the one-fluid, unstable case, as functions of the dimensionless surface tension parameter ζ^* for $k^* = k^*_{max}$.
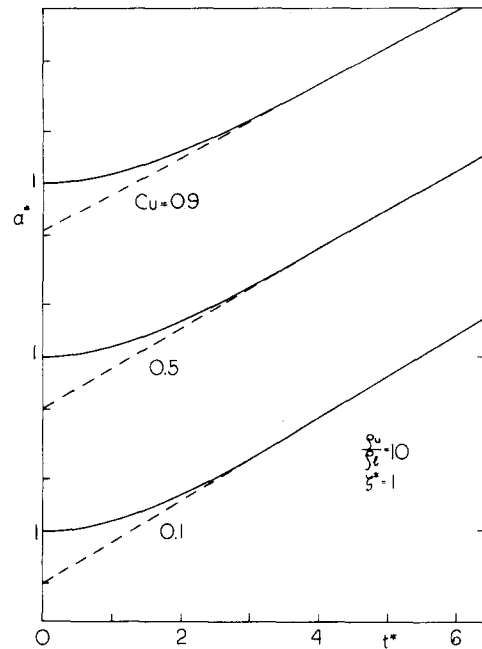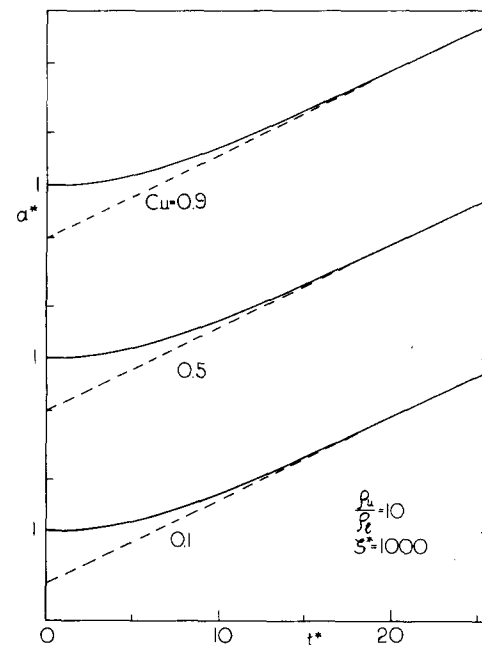

FIG. 6. The amplitude of the free surface motion in the unstable, two-fluid case [Eq. (22), continuous line] is compared with the asymptotic, normal mode result [Eq. (24), dashed line] for $a_0 = 1$, $u_0 = 0$, $\rho_u/\rho_l = 10$, $k^* = 0.346$, $\zeta^* = 1$, $C_u = 0.1$, 0.5, and 0.9.

tion with the growth rate of the normal-mode approach, i.e.,

$$a(t) \simeq \frac{\sigma_2 a_0 - u_0}{\sigma_2 - \sigma_1} e^{\sigma t}. \tag{31}$$

This equation is shown by the fourth line (dash and double dot) in Figs. 1–3 and is seen to be a rather poor

FIG. 7. The amplitude of the free surface motion in the unstable, two-fluid case [Eq. (22), continuous line] is compared with the asymptotic, normal mode result [Eq. (24), dashed line] for $a_0 = 1$, $u_0 = 0$ $\rho_u/\rho_l = 10$, $k^* = 0.0181$, $\zeta^* = 1000$, $C_u = 0.1$, 0.5, and 0.9.

approximation. To give an idea of the differences that can be expected between (31) and (24) in Fig. 5 we show graphs of the two multiplicative constants in front of the exponentials in Eqs. (24) and (31) as functions of ζ^* for $a_0 = 1$, $u_0 = 0$. In computing the quantities shown in Figs. 4 and 5, k^* has again been chosen on the basis of Eq. (29). Although in both figures the two curves tend to coalesce as $\zeta^* \to \infty$, it is seen that this happens very slowly. The marked differences between the exact result and the approximations (29) and (31) that can be observed in the small-viscosity example of Fig. 3 are a manifestation of this slowness in convergence.

Some results for the case in which the lower fluid also has non-negligible density and viscosity are shown in Figs. 6 and 7. These results have been computed by numerical inversion of $\bar{a}(s)$ given by (22) effected by means of the method of Ref. 23. The confluence of the numerical results (continuous lines) and the asymptotic ones, Eq. (24) (dashed lines) gives confidence in the accuracy of the numerical procedure. As already noted, in the two-fluid case no meaningful irrotational approximation exists, and accordingly, we do not have approximations corresponding to Eqs. (29) and (31) in this case.

Figure 6 refers to $\zeta^* = 1$, $a_0^* = 1$, $u_0^* = 0$, $\rho_u/\rho_l = 10$, $C_u = 0.1$, 0.5, and 0.9. In Fig. 7, $\zeta^* = 10^3$ while the other parameters have the same values. Although we have explored a much wider range of values of ζ^*, ρ_u/ρ_l, and C_u, we do not show further examples because the pattern observed is not different from that which appears from these figures. In all cases it was observed that the exact and asymptotic results merged as soon as the amplitude had grown by a factor of 3–6. As could be expected in view of the increased strength of the vorticity source at the interface introduced by the no-slip condition, this process proceeds at a somewhat faster rate than in the one-fluid cases shown previously, but the difference is very slight and perhaps affected by numerical inaccuracies.

The multiplicative constant of the asymptotic solution (24) is found to vary considerably in the range 0.4–0.8
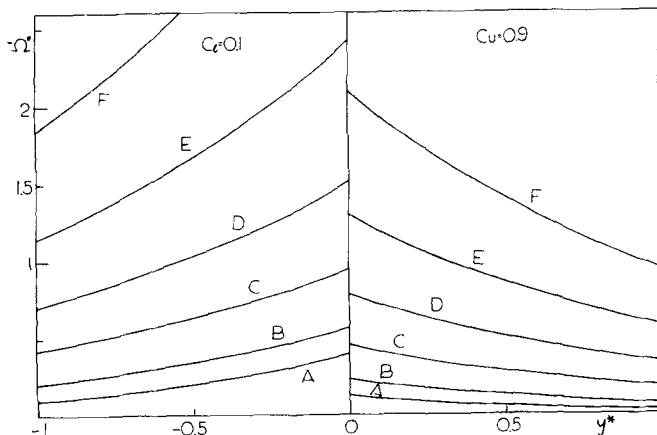
as the parameters A_l, A_u, C_l, C_u are varied, exhibiting, for $A_{l,u}$ fixed, a more or less pronounced maximum for intermediate values of $C_{l,u}$. For the sake of brevity, we do not present results similar to those of Fig. 5 for this quantity.

Finally, in Figs. 8 and 9 we show graphs of the dimensionless vorticity distribution in the two fluids obtained by numerical inversion of the results (17) at various instants of time. Both figures are for $\zeta^* = 1$, $\rho_l/\rho_u = 10$, $a_0^* = 1$, $u_0^* = 0$, Fig. 8 for $C_u = 0.9$, $C_l = 0.1$ and Fig. 9 for $C_u = 0.1$, $C_l = 0.9$. Naturally, the vorticity distribution is found to be much steeper in the fluid with lower viscosity. The value at the interface is also higher for the less viscous fluid, particularly when it is the upper one. This difference is evidently caused by the fact that in this case the velocity with which the upper fluid penetrates into the lower one is greater.

V. RESULTS: STABLE CASE

The advantage of the dimensionless variables used in the previous section stems essentially from the limited effect (demonstrated in Ref. 22) that the parameters $A_{l,u}, C_{l,u}$ have on several important quantities of the phenomenon once that they are expressed in terms of those variables. Since this matter has not been investigated for the stable case, there is no compelling reason to use the same nondimensional variables. The scaling which we now introduce renders the time scale of the process insensitive to the value of the surface tension parameter (as well as to differences in fluid densities) and introduces in a natural way the dimensionless quantity of Eq. (30). We take as fundamental time ω_0^{-1}, with ω_0 given by (16), and as fundamental length k^{-1} and we set

$$\tau = \omega_0 t, \quad \bar{\sigma} = \omega_0^{-1}\sigma, \quad \epsilon_{l,u} = \nu_{l,u}k^2/\omega_0. \tag{32}$$

It is straightforward to verify that all the preceding equations, and in particular (22) and (24), can be expressed in terms of these quantities and of ρ_l/ρ_u. Notice that, in this way, the wave number k no longer appears in the equations indicating, quantitatively, the
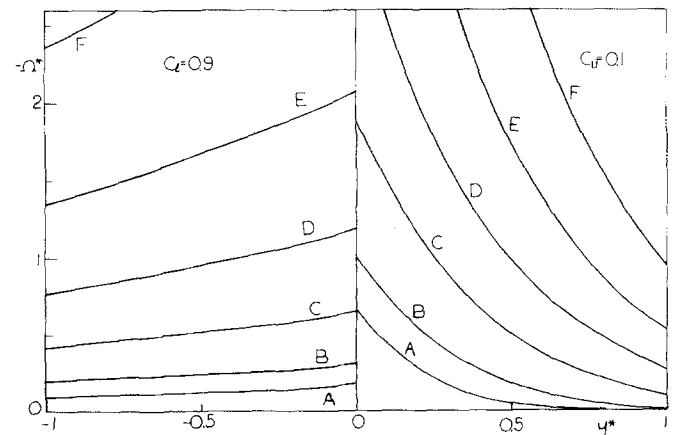

FIG. 8. The vorticity distribution in the two fluids, obtained by numerical inversion of Eq. (17), is shown at different instants of time for $a_0 = 1$, $u_0 = 0$, $\rho_u/\rho_l = 10$, $k^* = 0.346$, $\zeta^* = 1$, $C_u = 0.9$, $C_l = 0.1$, $\epsilon_u = 0.215$, $\epsilon_l = 0.239$. Curves A are for $t^* = 0.05$, B for $t^* = 0.1$, C for $t^* = 0.2$, D for $t^* = 0.3$, E for $t^* = 0.4$, F for $t^* = 0.5$.

FIG. 9. The vorticity distribution in the two fluids, obtained by numerical inversion of Eq. (17), is shown at different instants of time for $a_0 = 1$, $u_0 = 0$, $\rho_u/\rho_l = 10$, $k^* = 0.346$, $\zeta^* = 1$, $C_u = 0.1$, $C_l = 0.9$, $\epsilon_u = 0.0239$, $\epsilon_l = 2.15$. Curves A are for $t^* = 0.05$, B for $t^* = 0.1$, C for $t^* = 0.2$, D for $t^* = 0.3$, E for $t^* = 0.4$, F for $t^* = 0.5$.
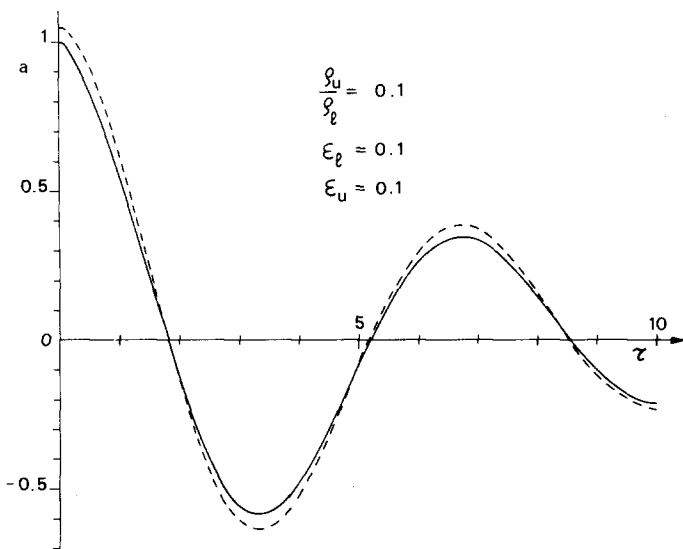
FIG. 10. The amplitude of the free surface wave in the stable case [Eq. (22), continuous line] is compared with the asymptotic, normal mode result [real part of Eq. (24), dashed line] for $a_0 = 1$, $u_0 = 0$, $\rho_u/\rho_l = 0.1$, $\epsilon_l = 0.1$, $\epsilon_u = 0.1$.
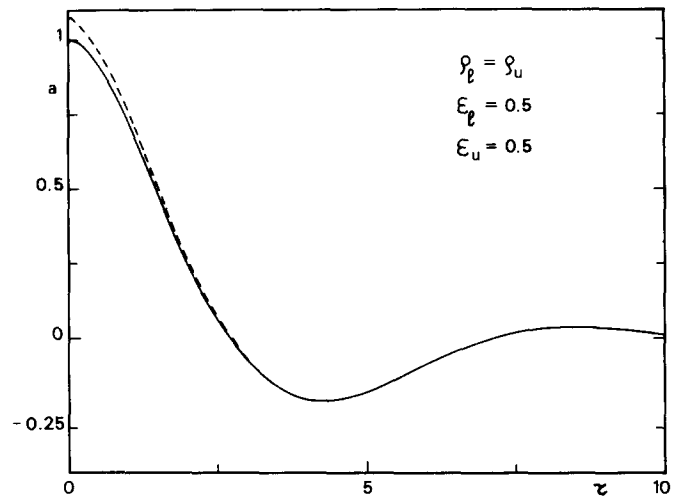
FIG. 11. The amplitude of the free surface wave in the stable case [Eq. (22), continuous line] is compared with the asymptotic, normal mode result [real part of Eq. (24), dashed line] for $a_0 = 1$, $u_0 = 0$, $\rho_u = \rho_l$, $\epsilon_l = 0.5$, $\epsilon_u = 0.5$.

balancing effect of increasing k and decreasing ν (for fixed ω_0). Thus, for example, if the scales in the figures of the previous section are altered in order to reflect the new dimensionalization those results can be referred to different fluids and different wavelengths. (Of course, $|\omega_0|^{-1/2}$ should be used in the unstable case rather than $\omega_0^{-1/2}$.)

Results for the one-fluid stable case have been presented in detail in Ref. 1 and will not be considered further. In Figs. 10 and 11 we show two examples of the surface oscillations obtained by numerical inversion of Eq. (22) (continuous line) compared with the asymptotic result (24) (dashed line) for $a_0 = 1, u_0 = 0$. Contrary to Ref. 1, agreement of the two results is not imposed for $t = 0$, but asymptotically for $t \rightarrow \infty$. In Fig. 10, $\rho_l/\rho_u = 10$, $\epsilon_l = \epsilon_u = 0.1$ and in Fig. 11 $\rho_l = \rho_u$, $\epsilon_l = \epsilon_u = 0.5$. Notice in the first example the slow confluence of the exact and asymptotic results relative to the unstable case. This difference can be traced to the fact that, for an oscillatory motion of the interface, the vorticity becomes a damped "wave" which propagates away from the interface (see Figs. 8 and 9 of Ref. 1), and thus the damping of the system is much smaller than in the unstable case. Of course, as shown in Fig. 11, this effect decreases as the viscosity of the system increases. For this stable configuration we have again obtained results for a wide range of parameter values, but no significant qualitative features different from those shown in Figs. 10 and 11 have been found.

ACKNOWLEDGMENTS

[1]A. Prosperetti, Phys. Fluids 19, 195 (1976).
[2]R. Menikoff, R. C. Mjolness, D. H. Sharp, C. Zemach, and B. J. Doyle, Phys. Fluids 21, 1674 (1979).
[3]G. F. Carrier and C. T. Chang, Q. Appl. Math. 16, 436 (1959).
[4]H. Lamb, Hydrodynamics (Cambridge University Press, Cambridge, England, 1932; reprinted by Dover, New York, 1945), 6th ed.
[5]S. Chandrasekhar, Hydrodynamic and Hydromagnetic Stability (Clarendon, Oxford, England, 1961).
[6]Lord Rayleigh, Proc. London Math. Soc. 14, 170 (1883); reprinted in Scientific Papers (Cambridge U. P., Cambridge England, 1900), Vol. 2, p. 200.
[7]W. J. Harrison, Proc. London Math. Soc. 6, 396 (1908).
[8]G. I. Taylor, Proc. R. Soc. London, Ser. A 201, 192 (1950).
[9]R. Bellman and R. H. Pennington, Q. Appl. Math. 12, 151 (1954).
[10]W. H. Reid, Proc. Cambridge Philos. Soc. 57, 415 (1961).
[11]L. D. Landau and E. M. Lifshitz, Quantum Mechanics (Addison-Wesley, Reading, Mass., 1959), Chap. 1.
[12]A. Prosperetti, Q. Appl. Math. 35, 339 (1977).
[13]A. Properetti, J. Méc. 19, 149 (1980).
[14]C. E. Grosch and H. Salwen, J. Fluid Mech. 87, 33 (1978).
[15]M. S. Plesset and C. Whipple, Phys. Fluids 17, 1 (1974).
[16]J. K. Dienes, Phys. Fluids 21, 736 (1978).
[17]E. Hameiri, Phys. Fluids 22, 89 (1979).
[18]G. K Batchelor, An Introduction to Fluid Dynamics (Cambridge U. P., Cambridge, England, 1970), p. 364.
[19]L. Cortelezzi and A. Prosperetti, Phys. Fluids (to be published).
[20]L. Cortelezzi and A. Prosperetti, Q. Appl. Math. (to be published).
[21]A. Prosperetti, J. Fluid Mech. 100, 333 (1980).
[22]R. Menikoff, R. C. Mjolness, D. H. Sharp, and C. Zemach, Phys. Fluids 20, 2000 (1977).
[23]F. Durbin, Comput. J. 17, 371 (1974).

1223   Phys. Fluids, Vol. 24, No. 7, July 1981

Andrea Prosperetti   1223